Research on Chemical Intermediates (2020) 46:1587–1611
https://doi.org/10.1007/s11164-019-04052-3

Design and synthesis of novel ditopic ligands with a pyrazole ring in the central unit

Bogdan-Ionel Bratanovici[1,2] · Alina Nicolescu[3] · Sergiu Shova[4] · Ioan-Andrei Dascălu[1] · Rodinel Ardeleanu[4] · Vasile Lozan[1,5] · Gheorghe Roman[4]

Received: 16 August 2019 / Accepted: 27 November 2019 / Published online: 3 December 2019

Abstract

Four novel ditopic ligands that have a pyrazole ring in their central unit and are useful for the generation of coordination polymers have been synthesized. Two of these ditopic ligands present two carboxylate functions as coordinating groups, while the other two are hybrid ligands having only one carboxylate function and either tetrazolate or imidazole as the remaining coordination site. The ligands have been obtained through a multi-step reaction sequence that begins with the Claisen condensation of either 4-acetylbenzonitrile or 4-(1*H*-imidazol-1-yl)acetophenone with diethyl oxalate and has the Knorr pyrazole ring closure as its key step. Subsequently, the tetrazolate in one of the ligands is constructed through a [3 + 2] cycloaddition of azide anion to the cyano group, while hydrolysis of the ester and the cyano substituents generates the carboxylate function(s). The structure of the intermediates and of the target ligands has been investigated by solution NMR, special attention being given to keto–enol and pyrazole tautomerism when present. The structure of two ligands and a key intermediate has also been established by single-crystal X-ray diffraction.

Electronic supplementary material The online version of this article (https://doi.org/10.1007/s11164-019-04052-3) contains supplementary material, which is available to authorized users.

✉ Gheorghe Roman
gheorghe.roman@icmpp.ro

[1] Centre of Advanced Research in Bionanoconjugates and Biopolymers (IntelCentru), Petru Poni Institute of Macromolecular Chemistry, 41A Aleea Gr. Ghica Vodă, 700487 Iasi, Romania

[2] Faculty of Chemistry, Alexandru Ioan Cuza University, 11 Bd. Carol, 700506 Iasi, Romania

[3] Department of Physics of Polymers and Polymeric Materials, Petru Poni Institute of Macromolecular Chemistry, 41A Aleea Gr. Ghica Vodă, 700487 Iasi, Romania

[4] Department of Inorganic Polymers, Petru Poni Institute of Macromolecular Chemistry, 41A Aleea Gr. Ghica Vodă, 700487 Iasi, Romania

[5] Institute of Chemistry of MECR, 3 Academiei Str., 2028 Chişinău, Republic of Moldova

Keywords Heterocycle · Pyrazole · Carboxylic acid · Ligand · Crystal structure

Introduction

Polytopic ligands, together with ions of multivalent metals, are the building blocks of coordination polymers. Because of their significant applications [1–4], a particular type of porous coordination polymers, generically called metal–organic frameworks (MOFs), has enjoyed the attention of numerous research groups in the last decades. For the construction of MOFs, the polytopic ligands that are used as organic linkers should be fairly rigid compounds in order to lead to bi- or tridimensional hollow structures sufficiently robust to retain the internal voids even after thermal activation and repeated cycles of gas adsorption–desorption [5]. From a structural point of view, these rigid organic linkers consist of a central unit (or core), which is either substituted with various functional groups that are able to coordinate to metal ions (such as carboxylate, sulfonate, or phosphonate), or feature coordinating sites based on nitrogen-containing heterocycles (*e.g.*, pyrazole, imidazole, triazole, tetrazole, pyridine, etc.). Commercially available, inexpensive terephthalic and isophthalic acids are frequent dicarboxylate organic linkers in MOFs, while trimesic acid is a well-known example of a broadly used tricarboxylate organic spacer in metal–organic networks. In fact, most of the organic linkers employed for the generation of coordination polymers have a central unit based either on a phenyl ring, a fused aromatic hydrocarbon-based ring system (naphthalene, anthracene, etc.), or an aromatic hydrocarbon-based ring assembly in whose structure the individual phenyl rings are joined through a single σ_{C-C} bond (such as polyphenyl scaffolds biphenyl or terphenyl, for example). Despite the fact that heterocyclic compounds represent almost two-thirds of all the known organic compounds, their presence as units in the make-up of the core of organic linkers used for the synthesis of MOFs is still limited. Again, commercially available, simple ligands such as thiophene-2,5-dicarboxylic acid [6, 7], furan-2,5-dicarboxylic acid [8, 9], pyridine-derived dicarboxylic acids [10, 11], or imidazole-4,5-dicarboxylic acid [12, 13] have started to be employed as organic linkers for MOFs, but the literature on this specific topic is still scarce compared to the volume of available information on MOFs based on organic linkers derived having an aromatic, entirely hydrocarbon-based central unit. As more research groups have started to design and synthesize their own organic linkers using conventional organic synthesis, the literature featuring MOFs that incorporate organic linkers with heterocyclic units in their cores has steadily increased. Design of organic linkers is critical for the preparation of MOFs with targeted structures and properties, and the replacement of carbocycles with heterocycles in the core of these ligands is expected to lead to novel and interesting coordination polymers. As a part of an ongoing project for the development of novel porous coordination polymers with organic ligands of variable length for gas storage [14–17], the current study outlines the preparation and characterization of several hitherto unknown ditopic carboxylate and hybrid ligands with a pyrazole ring in the central unit that are potentially useful for the generation of novel coordination polymers.

Results and discussion

Generally, the series of ligands reported in this paper have been designed by formally replacing a phenyl moiety in the biphenyl central unit of several well-known ditopic ligands with a pyrazole moiety. For example, starting from [1,1′-biphenyl]-4,4′-dicarboxylic acid and employing this simple methodology, the corresponding ligand to be obtained would have the general structure of 5-(4-carboxyphenyl)-1*H*-pyrazole-3-carboxylic acid. A valuable synthetic strategy for the generation of pyrazoles having a carboxyl function involves the ring closure of 4-aryl-2,4-dioxobutanoic acid esters with hydrazine derivatives [18]. The substituent in the aryl group in 4-aryl-2,4-dioxobutanoates, which are usually obtained from an aryl alkyl ketone through a Claisen condensation with ethyl oxalate, should be specifically chosen with the view to allow facile access to the second carboxyl function in the designed pyrazole-containing ligand. After close inspection of commercially available acetophenones, 4-acetylbenzonitrile **1** was selected as a convenient starting material for the preparation of the previously mentioned ditopic carboxylate ligand. The reaction sequence leading to the designed ligand is illustrated in Scheme 1.

Various synthetic variants for the Claisen condensation of 4-acetylbenzonitrile with diethyl oxalate, which usually differ from one another in terms of the combination solvent/base used in the preparation, reaction temperature or reaction time, are

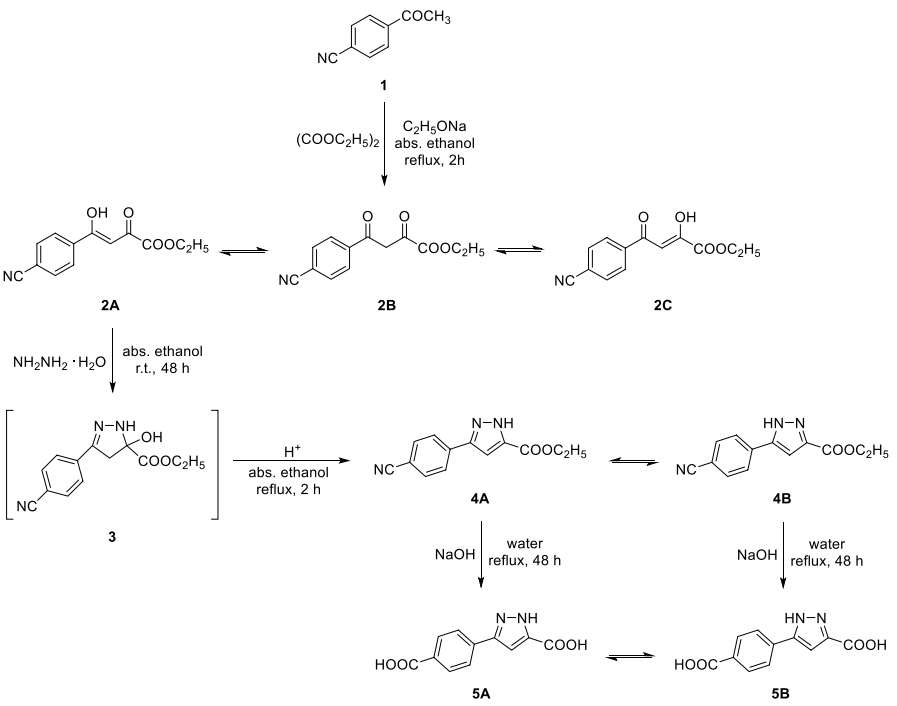

Scheme 1 Reaction sequence leading to 3(5)-(4-carboxyphenyl)-1*H*-pyrazole-5(3)-carboxylic acid **5**

available in the literature [19–22]. The procedure employed in this work has been adapted from Rogez-Florent et al. [22] and was found to reliably afford around 95% of the crude ethyl 4-(4-cyanophenyl)-2,4-dioxobutanoate (**2**), which can be conveniently purified through recrystallization from ethanol. However, this material incorporates a small amount of an impurity that is insoluble in ethanol, and attempts to remove it during the recrystallization stage through filtration of the hot, concentrated mixture are troublesome, as this operation usually resulted in the separation of the diketoester **2** on the filter paper as well. The removal of this impurity is more suitably performed by freely dissolving the diketoester in a small volume of cold chloroform, removal of the insoluble impurity through filtration, followed by the removal of chloroform from the filtrate to give a solid that is subsequently recrystallized from ethanol.

Although compound **2** appears as an intermediate in the synthesis of pyrazoles in the previously mentioned publications, its thorough characterization is still absent in the literature. Its IR spectrum (Fig. 1S in Supplementary Material) exhibits the expected $\boldsymbol{\nu_{C\equiv N}}$ band at 2226 cm^{-1} and ester $\nu_{C=O}$ at 1726 cm^{-1}, whereas the intense bands at 1690, 1610 and 1597 cm^{-1} could be attributed to vibrations of carbonyl in the keto tautomer and to vibrations of both carbonyl and ethylenic double bonds in the enol tautomer of compound **2** in solid state. NMR spectroscopy analysis has shed some light on the contribution of the three possible tautomeric forms to the structure of compound **2** in solution. In $CDCl_3$, the number of signals, their chemical shifts values and the ratio of integrals in the ^1H NMR spectrum of **2** (Fig. 2S in Supplementary Material) suggest the absence of the keto tautomer **2B**, while the sharp singlet at 7.03 ppm and the broad signal centered at approximately 15 ppm are, however, indicative of an enol form. According to the literature data, the enol form of β-diketones is generally preferred in solution to the keto form, owing to the strong intramolecular hydrogen bond which stabilizes the enol form as a six-membered chelate ring [23, 24]. In these experimental conditions, only one set of signals was observed in the NMR spectra for the enolic tautomer, presumably because of the rapid interconversion between enol forms **2A** and **2C**. As a consequence, the recorded proton and carbon NMR spectra of compound **2** correspond to the weighted average of the two forms **2A** and **2C**, in which a single resonance for each type of nuclei of the non-symmetric enol forms is present. The presence of the enol form in $CDCl_3$ is also substantiated by the signals at 98 ppm and 187 ppm in the ^{13}C NMR spectrum of **2** (Fig. 3S in Supplementary Material), which are characteristic for enols. The discrimination and exact assignment of the signals for the two magnetically non-equivalent carbon atoms in the keto–enol fragment of compound **2** were gleaned from the HMBC spectrum (Fig. 4S in Supplementary Material) and were based on the three-bond correlation between the carbon atom in the carbonyl adjacent to the phenyl ring and the aromatic protons.

In the next stage, reaction of compound **2** with hydrazine was employed to construct the pyrazole ring substituted with the ester function (Scheme 1). Initially, the diketoester was heated in absolute ethanol at reflux temperature with a 1.5-fold excess of hydrazine hydrate for 7 h. NMR analysis of the isolated material showed that it was a mixture of the hydrazide related to ester **4** and the desired ester **4** (ratio approximately 6 to 1, respectively). A second attempt at obtaining ester **4**

was performed under milder conditions and entailed reacting equimolar amounts of diketoester and hydrazine hydrate in absolute ethanol at room temperature for 48 h. The isolated material consisted of a mixture of the desired ester **4** and hydroxypyrazoline **3**, according to the ^{1}H NMR spectrum (Fig. 5S in Supplementary Material). The existence of hydroxypyrazoline **3** is supported by the presence in this spectrum of two doublets at 3.14 ppm and 3.52 ppm, characteristic for diastereotopic protons in the methylene group of the pyrazoline ring. In addition, the existence in the carbon spectrum of this mixture of peaks at approximately 43 and 92 ppm that are specific to hydroxypyrazoline **3** further substantiates the presence of this intermediate (Fig. 6S in Supplementary Material). Formation and even isolation of hydroxypyrazolines as intermediates in the cyclocondensation of β-diketones with hydrazine derivatives have been reported often [25–27]. Two potential hydroxypyrazoline could arise from the reaction of non-symmetrical diketoester **2** with hydrazine, but correlation spectroscopy strongly supports for hydroxypyrazoline **3** the particular structure in which the hydroxyl and ester functions are geminal. Thus, close inspection of the HMBC spectrum of the mixture of ester **4** and hydroxypyrazoline **3** (Fig. 7S in Supplementary Material) revealed a three-bond correlation between the sp^2 carbon atom of hydroxypyrazoline (145.60 ppm) and the aromatic protons in the phenyl moiety.

In order to obtain the fully aromatized pyrazole, the mixture consisting of the desired ester **4** and hydroxypyrazoline **3** was further refluxed in absolute ethanol, in the presence of a catalytic amount of concentrated H_2SO_4 as dehydrating agent, for 2 h. The isolated product was practically the pure ester **4**, as NMR analysis confirmed. Preparation of ester **4** from compound **2** was also examined as a one-pot reaction under the conditions that have previously been shown to lead to the target compound in two steps. Therefore, after the mixture of diketoester **2** and hydrazine had been stirred at room temperature for 48 h, sufficient conc. H_2SO_4 was added in order to render it acidic (pH 1–3), and the mixture was then heated at reflux temperature for 2 h to afford practically pure ester **4** in 65% yield.

As a non-symmetrically 3,5-disubstituted pyrazole, compound **4** could also be theoretically conceived as a mixture of two tautomers **4A** and **4B** (Scheme 1). NMR analysis of a sample of ester **4** confirmed experimentally the presence of these two tautomers in solution. The sharp signals visible for each tautomer in both ^{1}H and ^{13}C NMR spectra (Fig. 8S and 9S in Supplementary Material) indicate the existence of a slow exchange between the two forms, the lifetime of each tautomer being longer than $1/\Delta\delta$ (where $\Delta\delta$ represents the chemical shift difference between the corresponding signals of each tautomeric form). In ^{13}C NMR spectrum, each tautomer has a characteristic signal that allows for their discrimination. Thus, the signal at 149.57 ppm corresponds to C-3 carbon from the pyrazole ring, in tautomer **4A**, an assignment that is supported by the three-bond correlation signal obtained in H,C-HMBC spectrum (Fig. 10S in Supplementary Material) between the aromatic protons H-2′ and the quaternary pyrazole carbon C-3. From the same type of three-bond correlation, C-5 in tautomer **4B** was attributed the signal at 141.74 ppm. Similar chemical shift values for C-3/C-5 were reported in previous studies of tautomerism of 3(5)-phenyl-*1H*-pyrazoles [28] and phenylene-bis(pyrazole) derivatives [29] using both solid NMR and solution NMR. The exact assignment for all the protons

and carbons in the two tautomeric forms was based on the correlations obtained from the two-dimensional experiments, such as H,H-COSY, H,C-HSQC, and H,C-HMBC. The comparison of the integration of the signals corresponding to the same type of proton in tautomers **4A** and **4B** yields a ratio of 1 to 0.6 between the respective tautomers. The IR spectrum of pyrazole **4** (Fig. 11S in Supplementary Material) presents the specific stretching vibration bands $\boldsymbol{\nu}_{\mathbf{C\equiv N}}$ at 2228 cm^{-1} and ester $\nu_{C=O}$ at 1713 cm^{-1}.

In the final step, compound **4** was converted to diacid **5** through alkaline hydrolysis of both cyano and ester functions. Because conversion of a nitrile group to carboxylate normally requires harsher conditions than the transformation of an ester function to carboxylate, compound **4** was heated at reflux temperature in water in the presence of excess NaOH for 48 h with the view to ensure the complete hydrolysis of the cyano group. The initial suspension gradually turned into a colorless solution as the ester hydrolysis progressed. Finally, the reaction product was isolated by bringing the pH of the solution to 5–6 with dilute acetic acid.

From a theoretical point of view, diacid **5** could also be conceived as a pair of tautomers **5A** and **5B** (Scheme 1). Nonetheless, NMR analysis of diacid **5** in solution revealed only one set of signals, which suggests that the slow interconversion of tautomers identified for ester **4** does not take place in the case of diacid **5**. This dissimilar behavior made the attribution of the signals from the ^{1}H NMR spectrum of diacid **5** (Fig. 12S in Supplementary Material) easier than it was for ester **4**. However, several signals corresponding to different quaternary carbons were not discernible in the ^{13}C NMR, most likely because of a severe line broadening, which is a characteristic for an intermediate exchange condition [28]. Because it would have been difficult to confirm the chemical structure of diacid **5** beyond any doubt without the identification of all expected signals in the carbon spectrum, an additional NMR experiment was performed with the same sample. Thus, hoping to disrupt the interconversion of the tautomers and freeze the molecules of **5** as a single, protonated species, 2 drops of non-deuterated trifluoroacetic acid (TFA) were added to the initial solution of diacid **5** in DMSO-d_6, and then, the proton and carbon spectra were recorded one more time. The addition of TFA did not chemically modify the structure of diacid **5** (as proved by the proton spectrum, Fig. 13S in Supplementary Material), yet it led to sharper signals in carbon spectrum, allowing the identification of all of the expected carbon signals (Fig. 14S in Supplementary Material). In-depth analysis of the solution behavior of the synthesized pyrazole derivatives is beyond the scope of this work; therefore, no additional NMR experiments, including (but not restricted to) measurements at variable temperature or in other NMR solvents, have been performed. The exact assignments, particularly for the peaks in the ^{13}C NMR spectrum, were inferred from HSQC and HMBC experiments, the latter being especially useful in ascribing the signals for carbon atoms at positions 3 and 5 of pyrazole ring and in the two carboxylic groups using three-bond correlations. The IR spectrum of diacid **5** showed a very intense band at 1672 cm^{-1}, which was assigned to $\nu_{C=O}$ in the carboxyl function (Fig. 15S in Supplementary Material).

Because *NH*-pyrazoles themselves are well-known ligands for the synthesis of complexes and coordination polymers [30–32], ligand **5** could theoretically act as a tridentate ligand. Therefore, it was considered interesting to synthesize an

N^1-substituted version of ligand **5** as well, with the view to compare the coordination mode of both ligands. Phenylhydrazine was chosen as the hydrazine derivative for the Knorr ring closure reaction with diketoester **2** to afford pyrazole **6** (Scheme 2). The dehydrative cyclocondensation was conducted in refluxing glacial acetic acid and usually afforded the crude pyrazole in yields greater than 90%. The isolation of the reaction product by dropwise addition of the reaction mixture onto water and ice under efficient stirring frequently led to the initial separation of a sticky semisolid that turned into a solid after had been kept in contact with the liquid medium for up to 48 h at room temperature, although, in a few occasions, a solid, finely dispersed material separated straightforwardly when the reaction mixture was poured onto ice–water. The NMR analysis of the crude material showed that it contained both regiosomers that could potentially arise from the reaction of phenylhydrazine with either of the oxo functions that are present in the structure of diketoester **2**, an issue that has been noticed in similar ring closure reactions [33–35]. It is common knowledge that the proton at C-4 of the pyrazole ring in the 1,5-diaryl isomer resonates upfield with respect to the corresponding signal of the 1,3-diaryl regioisomer [35]. Based on the ratio of the areas of the singlets corresponding to the proton at C-4 in both regioisomers in our mixture, the 1,5-diaryl isomer **6** ($\delta = 7.31$ ppm) represents 85–90% of the mixture, whereas the 1,3-diaryl regioisomer ($\delta = 7.79$ ppm) makes up for the rest. Similar mixtures of regioisomeric pyrazoles have been successfully separated using column chromatography [35]. However, because we required large amounts of this key intermediate in the preparation of ligands to be subsequently employed in the synthesis of coordination polymers, an exploration toward a more facile approach for the isolation of pure **6** from this mixture seemed reasonable. It was found out that in our case the 1,3-diaryl isomer could be removed without difficulty after two recrystallizations from ethanol, while allowing a good recovery of the desired pyrazole **6**. The characteristic stretching vibration bands $\boldsymbol{\nu}_{\mathbf{C\equiv N}}$ (2230 cm^{-1}) and ester $\nu_{C=O}$ (1711 cm^{-1}) are noticeable in the IR spectrum of intermediate **6**

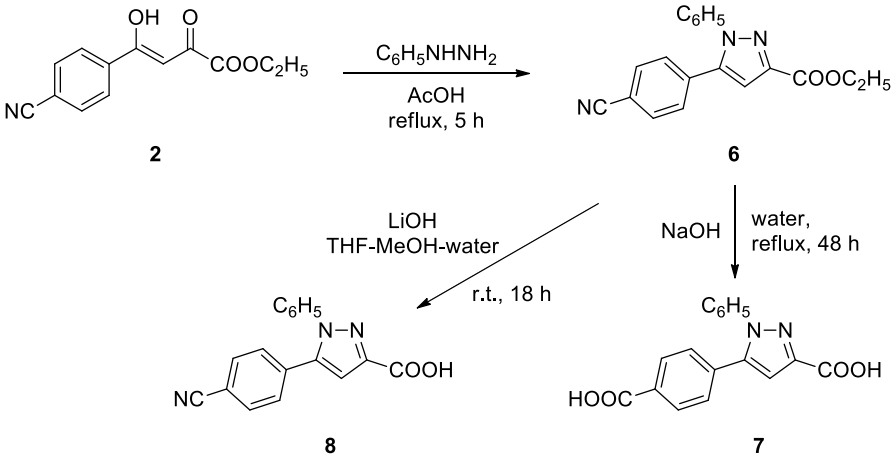

Scheme 2 Synthesis of intermediate **6** and its conversion into acids **7** and **8**

(Fig. 16S in Supplementary Material). Structural characterization by NMR spectroscopy of the pure compound **6** indicated the presence of a single species, characterized by sharp and well-defined signals in both proton and carbon spectra (Fig. 17S and 18S in Supplementary Material). The chemical shifts values for the quaternary carbons in the pyrazole ring (C-5 at 142.61 ppm and C-3 at 143.67 ppm) serve as additional proof for the structure of **6** as the 1,5-diaryl isomer.

In order to prove beyond any doubt that the key intermediate **6** is the 1,5-diaryl isomer, its structure has been also investigated using single-crystal X-ray diffraction technique. Single crystals suitable for diffraction were obtained through the slow evaporation at room temperature of a solution of ester **6** in ethanol. This pyrazole derivative crystallizes in *P*-1 space group of triclinic system with one neutral molecule as the asymmetric part of the unit cell (Fig. 1). No co-crystalized solvate molecules have been found in the structure. The structure determined by this method corresponds indeed to the 1,5-diaryl isomer. It is worth mentioning that the structure of compound **6** is closely related to a previously reported structure of an analogue having a chloro substituent instead of cyano [36]. In the crystal, the neutral molecules are interacting through C–H···O and C–H···N hydrogen bonding to form a one-dimensional supramolecular motif running along 101 direction, as shown in Fig. 2.

Alkaline hydrolysis of compound **6** having an ester function and a cyano group in its structure was conducted under the same conditions previously employed for the hydrolysis of its analogue **4** (Scheme 2). Thus, good yields of diacid **7** were obtained by refluxing nitrile–ester **6** for 48 h in an excess of dilute aqueous NaOH. The initial suspension gradually turned into a homogenous reaction mixture as the ester hydrolysis produced the water-soluble nitrile–acid sodium salt. At the end of the reaction time, diacid **7** was isolated by treating the cold, filtered reaction mixture with dilute HCl. The stretching vibration band $\nu_{C\equiv N}$ is no longer present in the IR spectrum of compound **7**, while the intense band at 1686 cm^{-1} could be attributed to $\nu_{C=O}$ in the

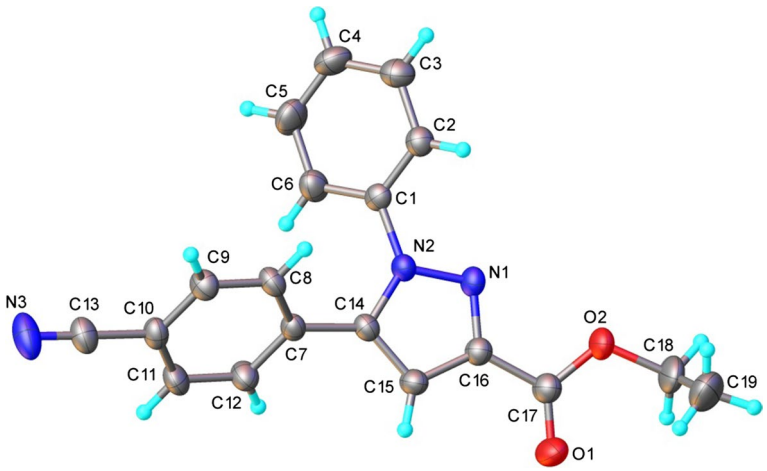

Fig. 1 X-ray molecular structure of pyrazole **6** along with atom labeling scheme and thermal ellipsoids at 50% probability level

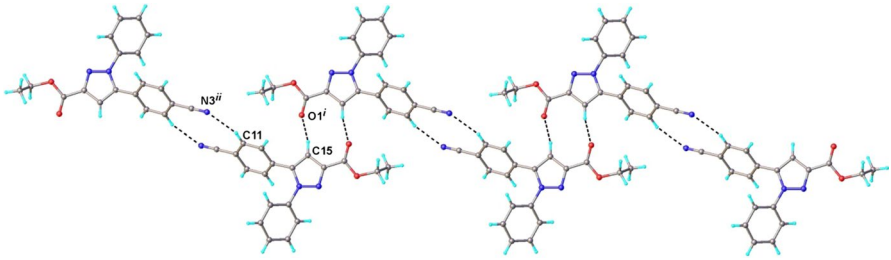

Fig. 2 A partial view of the 1D supramolecular chain in the crystal structure of **6**. H-bonds are shown in dashed black lines. H-bonds parameters: C11-H···N3 [C11-H 0.93 Å, H···N3 2.50 Å, C11-H···N3(3 − *x*, 1 − *y*, 2 − *z*) 3.385(2) Å, ∠C11HN3 159.0°]; C15-H···O1 [C15-H 0.93 Å, H···O1 2.55 Å, C15-H···O1(2 − *x*, 1 − *y*, 1 − *z*) 3.325(2) Å, ∠C15HO1 140.9°]

carboxyl function (Fig. 19S in Supplementary Material). The presence in the offset of the ^{1}H NMR spectrum of compound **7** of a broad singlet integrating for two protons (Fig. 20S in Supplementary Material), corroborated with the peaks at 162.89 and 166.71 ppm in its ^{13}C NMR spectrum (Fig. 21S in Supplementary Material), confirmed the complete and successful hydrolysis of both the ester function and the cyano group.

The long reaction and the relatively harsh conditions used for the alkaline hydrolysis of compound **6** have prompted us to explore a more mild approach toward the simultaneous transformation of the cyano and ester groups in this compound's structure into carboxylate. Thus, a method that has been initially used for the hydrolysis of esters of isoxazole-3-carboxylic acids [37] has been also contemplated for the hydrolysis of compound **6**. While the overnight reaction of nitrile–ester **6** with LiOH in a mixture of tetrahydrofuran (THF), methanol and water at room temperature proved efficient for the hydrolysis of the ester function at position 3 of the pyrazole ring, it left the cyano group unaffected and afforded the monoacid **8** as the only product (Scheme 2). IR analysis of this product (Fig. 22S in Supplementary Material) showed that the cyano function was still present ($\nu_{C\equiv N} = 2226$ cm^{-1}), while the ester group was converted into carboxyl ($\nu_{C=O} = 1676$ cm^{-1}). The course of the hydrolysis was also validated by NMR. Compared to diacid **7**, the proton spectrum of monoacid **8** (Fig. 23S in Supplementary Material), presented the same offset broad singlet, but the signal integrated only for one proton in this instance. In the ^{13}C NMR spectrum of monoacid **8** (Fig. 24S in Supplementary Material), the single peak with a chemical shift value higher than 160 ppm was associated with the carbon atom in the pyrazole carboxylate group, while the peak corresponding to the carbon atom of the cyano group was still noticeable at approximately 118 ppm.

Besides di- or polytopic carboxylic ligands, hybrid ligands containing in their structure one or several carboxylate functions along with one or more coordinating sites based on nitrogen-containing heterocycles are often used for the preparation of coordination polymers [38–42]. Therefore, we were also interested in the development of similar hybrid ligands having a pyrazole ring in the central unit. The presence of a cyano group in the structure of the key intermediate **6** opens the possibility for the synthesis of such a hybrid tetrazolate–carboxylate ligand using established

tetrazole chemistry (Scheme 3). Thus, the reaction of nitrile–ester **6** with NaN_3 in *N*,*N*-dimethylformamide (DMF) in the presence of NH_4Cl was employed for the conversion of the cyano into a tetrazole ring, using an adapted version of a method that previously proved successful for a series of simpler aromatic nitriles [43]. The [3 + 2] cycloaddition of the azide to the cyano group under these harsh reaction conditions is accompanied by the partial conversion of the ester function into carboxylate. Thus, in an initial experiment, only about half of the theoretical amount of the desired tetrazole–ester **9** was isolated as a solid material after the cold reaction mixture had been poured into a large volume of water. When the filtrate from the isolation of compound **9** was brought to pH 2–3 with dilute HCl, a second crop of a solid material was isolated; its analysis by ^{1}H NMR showed that it was a mixture of tetrazole–ester **9** and tetrazole–acid **10**, in the approximate ratio of 9 to 1, respectively, from which the former could be obtained, if desired, through recrystallization from ethanol. In a subsequent experiment, the suspension obtained after the cold reaction mixture had been poured onto water was directly treated with dilute HCl until pH reached 2–3 to afford a solid material which consisted mostly of tetrazole–ester **9** (90–95% purity) contaminated with tetrazole–acid **10**.

The absence of the stretching vibration band associated with the cyano group in the IR spectrum of compound **9** is indicative for the successful tetrazole ring closure, while the stretching vibration band of the carbonyl in the ester function is still present (Fig. 25S in Supplementary Material). The ^{1}H NMR spectrum of tetrazole–ester **9** (Fig. 26S in Supplementary Material), recorded in DMSO-d_6, is very similar to that of starting material **6**, and only the minor shift upfield of the δ value for the H-3′ protons and the presence of the tetrazole proton in offset provided an indication for the conversion of compound **6** into the desired tetrazole–ester **9**. Despite the potential annular prototropic tautomerism of the tetrazole ring [44], a single set of signals is present in the proton spectrum of compound **9**. The majority of the signals expected to be found in the ^{13}C NMR spectrum of **9** (Fig. 27S in Supplementary Material) were sharp, and

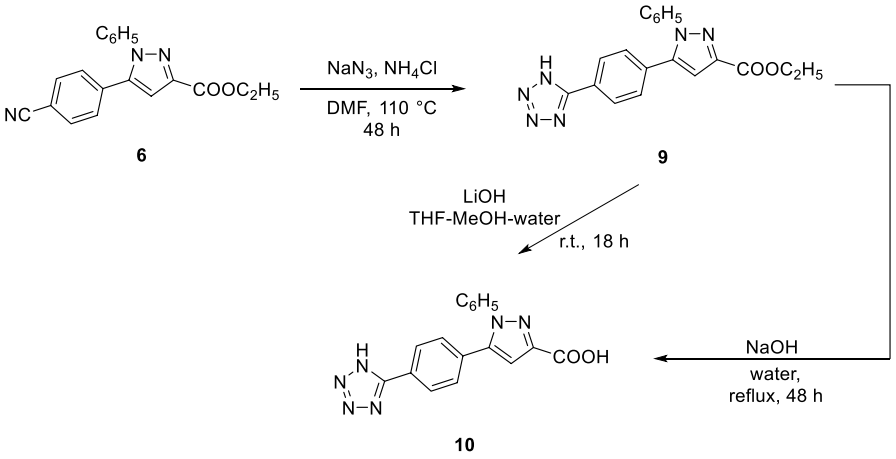

Scheme 3 Synthesis of tetrazole–acid **10**

their assignment was quite straightforward owing to the resemblance of the carbon spectrum of tetrazole–ester **9** to that of starting material **6**. Close inspection of the ^{13}C NMR spectrum led, however, to the discovery of a broadening (*i.e.*, a linewidth of 10 Hz, while other quaternary signals had 3–4 Hz) of the signal assigned to the quaternary C-4′ of the *para*-disubstituted benzene ring. In addition, a significant broadening of the signal assigned to the carbon atom in the tetrazole ring (C-5‴) was also identified. These findings suggest that an intermediate exchange involving the 1*H*-tautomer and the 2*H*-tautomer of tetrazole might occur, which is a process similar to that hypothesized for the N-1 unsubstituted pyrazole ring in diacid **5**. Although the broadening of the C-5‴ peak is so severe that the signal had been initially overlooked in the analysis of the carbon spectrum of **9**, the three-bond correlation between this atom ($\delta = 155.05$ ppm) and H-3′ from the *para*-disubstituted phenyl moiety ($\delta = 8.00$ ppm) in H,C-HMBC spectrum (Fig. 28S in Supplementary Material) led to its identification. It is worth mentioning that the chemical shift value for C-5‴ in an analog with a similar structure was 155.1 ppm [45]. The successful assignment of a signal to C-5‴ and the absence of the peak for the carbon atom of the cyano group in the carbon spectrum recorded for compound **9** undeniably confirmed the formation of the tetrazole ring.

Both the pure tetrazole–ester **9** and the mixture isolated directly from the cycloaddition reaction (which contains tetrazole–ester **9** as the major component and the desired hybrid ligand **10** as a minor component) have been used in the subsequent alkaline hydrolysis of the ester function to carboxylate. Heating either of these materials in aqueous NaOH at reflux temperature for 10 h (Scheme 3) leads to samples of tetrazole–acid **10** having practically the same high purity, as proved by NMR analysis. In addition, the milder hydrolysis approach (LiOH in THF–methanol–water at room temperature) that was successfully used for the hydrolysis of the ester function in compound **6** was also evaluated for the hydrolysis of tetrazole–ester **9** (Scheme 3) and found to provide access to ligand **10** with yields and purity that are comparable to the hydrolysis procedure performed in water at reflux temperature. A comparison between the IR spectra of compounds **9** and **10** shows that in the latter (Fig. 29S in Supplementary Material) the absorption band associated with the ester function has disappeared, while a sharp intense band assigned to the stretching vibration band of the carbonyl in the carboxyl group is noticeable at 1674 cm^{-1}. The structure of tetrazole–acid **10** has been further investigated by NMR spectroscopy. The aromatic region of the proton spectrum of acid **10** (Fig. 30S in Supplementary Material) is very similar to that of ester **9**, but the lack of signals in the aliphatic region and the presence of a broad singlet at approximately 13 ppm confirmed the hydrolysis of ester **9** to acid **10**. No peaks were found in the aliphatic region of the carbon spectrum of acid **10** as well (Fig. 31S in Supplementary Material), and all of the signals in the aromatic region of the same spectrum have been accounted for.

A structure in the solid state has been determined for this hybrid ligand through single-crystal X-ray diffraction. X-ray-quality single crystals of tetrazole–acid **10** were obtained by allowing the compound to slowly crystallize from its solution in DMSO–water (3:1, *v*/*v*) that was being kept at 80 °C. According to the data, tetrazole–acid **10** crystalizes in the Sohnke $P2_12_12_1$ space group of monoclinic system and exhibits a molecular crystal structure based on neutral entity, as shown in Fig. 3. No co-crystalized solvate molecules have been found in the structure. The crystal

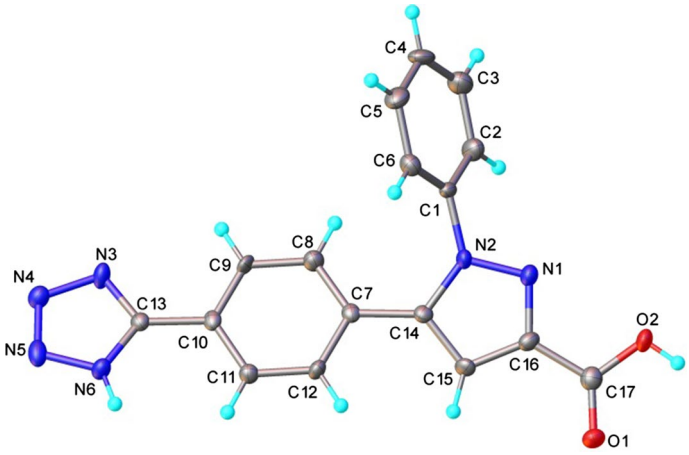

Fig. 3 X-ray molecular structure of compound **10** along with atom labeling scheme and thermal ellipsoids at 50% probability level

packing features N–H···O and O–H···O intermolecular hydrogen bonding, which determines the formation of a three-dimensional supramolecular architecture, as depicted in Fig. 4.

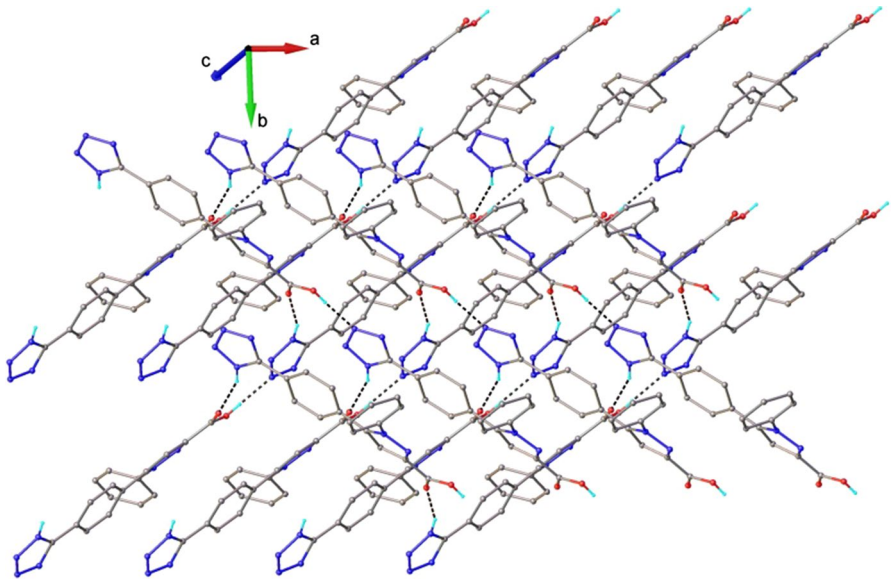

Fig. 4 Partial crystal packing diagram in the crystal structure of **10** showing 3D supramolecular network. Non-relevant H-atoms were omitted for clarity. H-bonds parameters: O2-H···N4 [O2-H 0.82 Å, H···N4 1.89 Å, O2-H···N4(2 + *x*, *y* − 1, *z*) 2.708(5) Å, ∠O2HN4 171.2°]; N6-H···O1 [N6-H 0.86 Å, H···O1 2.01 Å, N6-H···O1(− 1.5 + *x*, 0.5 − *y*, 1 − *z*) 2.815(5) Å, ∠N6HO1 155.6°]

Hybrid ligand **10** can act as a dianionic ligand in the synthesis of coordination polymers. In addition, we wanted to develop a hybrid ligand having a neutral *N*-donor site and an anionic *O*-donor coordination site grafted on a central unit containing a pyrazole ring. If the carboxylate on the pyrazole ring is being preserved as the anionic *O*-donor coordination site, this novel hybrid ligand can be formally derived from ligand **10** by replacing the tetrazole ring with an imidazol-1-yl moiety, for example. The key step in the synthetic strategy toward this ligand would also rely on the construction of the carboxyl-substituted pyrazole ring from a suitably substituted diketoester, in a manner similar to the approach used for the preparation of ligands **5**, **7** or **10**. Starting from commercially available 4-(1*H*-imidazol-1-yl)acetophenone (**11**), the reaction sequence leading to this hybrid ligand is outlined in Scheme 4. The other possible tautomers of diketoester **12**, which are similar to those of diketoester **2** in Scheme 1, have been omitted for clarity.

Ethyl 4-[4-(1*H*-imidazol-1-yl)phenyl]-2,4-dioxobutanoate (**12**) required for the ring closure to pyrazole was conveniently obtained through a typical Claisen condensation of 4-(1*H*-imidazol-1-yl)acetophenone (**11**) with diethyl oxalate. The reaction proceeds smoothly to afford the desired compound with good yields. The crude product is sufficiently pure to be used directly in the next step. The IR spectrum (Fig. 32S in Supplementary Material) has two intense absorption bands at 1755 cm^{-1} ($\nu_{C=O}$ in ester) and 1603 cm^{-1} ($\nu_{C=O}$ in the keto–enol system). NMR investigation of the analytical sample in $CDCl_3$ (Fig. 33S and 34S in Supplementary Material) showed that the enol tautomer is the preferred form in solution based on the signals for the characteristic protons (vinylic CH and enolic OH) and typical peak for the enolic carbon ($\delta = 97.7$ ppm) in the corresponding spectra.

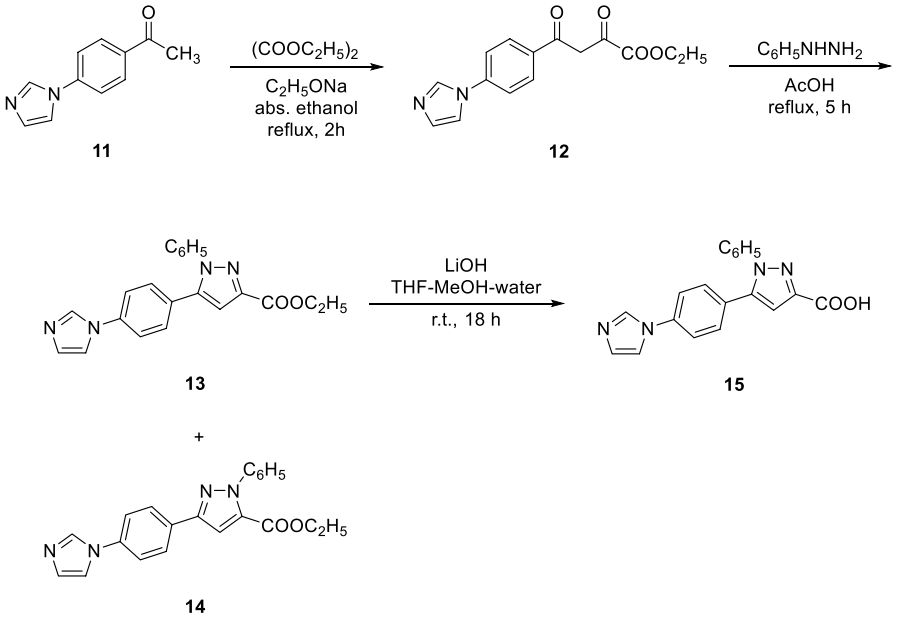

Scheme 4 Preparation of the imidazole-containing hybrid ligand **15**

The key step leading to ligand **15** is the construction of the carboxylate-substituted pyrazole ring through the reaction of diketoester **12** with phenylhydrazine in glacial acetic acid. The isolation of reaction product was achieved by bringing the reaction mixture, which had been previously diluted with ice–water, to pH 8 using dilute NaOH. Close inspection by NMR showed that this crude material was a mixture of regioisomers **13** and **14** in an approximate ratio of 9 to 1. The regioisomers could be separated by column chromatography to yield pyrazole **14** as the faster eluting component, followed by pyrazole **13** as the slower eluting compound. Because of the small difference between their R_f values, the separation is not particularly good, leading to fractions which contain both compounds. Consequently, the cumulate yield of both isomers after separation was only 68%. NMR analysis of these regioisomers (Fig. 36S–40S in Supplementary Material) confirmed that pyrazole **13** is the 1,5-diaryl isomer, while pyrazole **14** is the 1,3-diaryl isomer. Thus, the chemical shift value for the proton at C-4 in the pyrazole ring in **13** ($\delta = 7.09$ ppm) is upfield from the chemical shift value for the proton at C-4 in the pyrazole ring in **14** ($\delta = 7.35$ ppm). In addition, the chemical shift values for the quaternary carbon atoms C-3 and C-5 in the pyrazole ring were examined. For regiosomer **13**, these values are only slightly apart (which is typical for 1,5-diaryl pyrazoles), while in the case of regioisomer **14** the difference between these values is 15 ppm. In their IR spectra (Fig. 35S and 38S in Supplementary Material), both regioisomers have an intense absorption band close to 1700 cm^{-1} ($\nu_{C=O}$ in ester).

The isolation of pure target compound **13** from the mixture of regioisomers obtained in an identical synthetic experiment was also attempted through recrystallization from a small volume of 2-propanol. The recovery of pure ester **13** (as shown by the melting point and proton NMR, which were identical to those of the sample of **13** isolated through chromatography) was only 10%. Because this method was deemed unsatisfactory, a different approach, based on the property of imidazoles to form salts, was also examined using the mixture of regioisomers recovered from the recrystallization attempt. Thus, after 2-propanol was removed under reduced pressure, the mixture of regioisomers was dissolved in THF, and ethereal HCl was added to the solution until precipitation of hydrochlorides was complete. Repeated recrystallization of this mixture of hydrochlorides from abs. ethanol with the view to remove the unwanted isomer finally allowed the isolation of pure **13**·HCl, albeit with a modest recovery (30%). NMR analysis of the hydrochloride (Fig. 41S and 42S in Supplementary Material) confirmed its purity. Therefore, this method could constitute an alternative to chromatographic separation toward the isolation of pure intermediate **13**.

Hydrolysis of imidazole–ester **13**, either as the free base or as the hydrochloride, afforded the target ligand **15**. Based on our previous experience with the hydrolysis of tetrazole–ester **9**, the mild approach employing LiOH as base and taking place at room temperature was preferred to the procedure using a stronger base at reflux temperature. In the IR spectrum (Fig. 43S in Supplementary Material), the stretching vibration band of the carbonyl in the carboxyl group is present at 1690 cm^{-1}. The successful conversion of ester **13** into acid **15** is also supported by the presence in the offset of the proton spectrum of latter compound of a broad signal integrating for one proton (Fig. 44S in Supplementary Material) and also by the absence of any

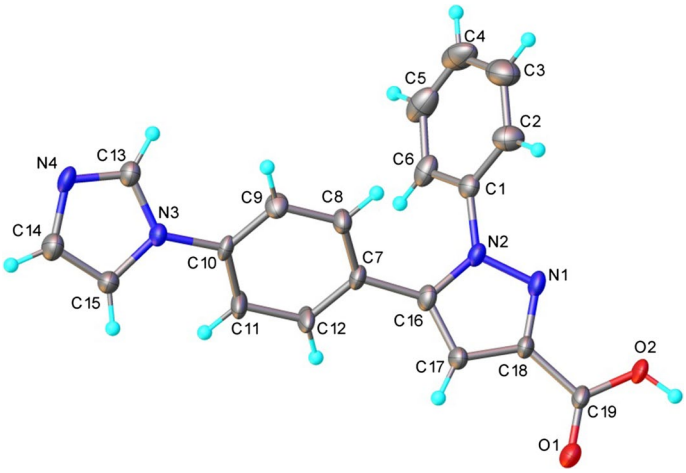

Fig. 5 X-ray molecular structure of compound **15** along with atom labeling scheme and thermal ellipsoids at 50% probability level

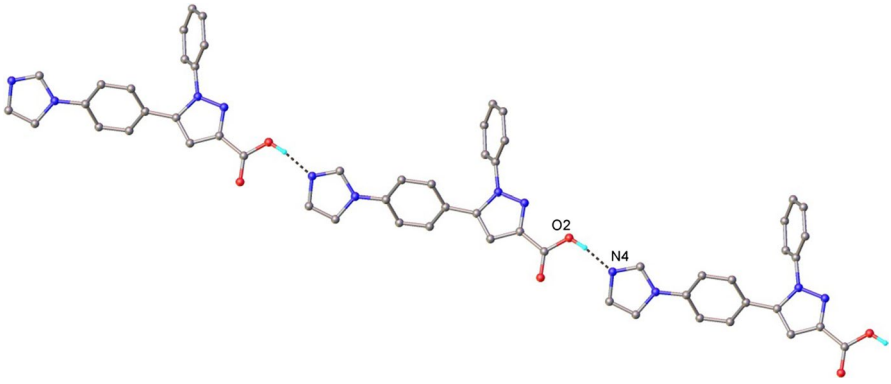

Fig. 6 View of 1D supramolecular chain in the crystal structure of imidazole–acid **15**. H-bond parameters: O2-H···N4 [O2-H 0.87 Å, H···N4 1.71 Å, O2-H···N4(x, $y-1$, z)

signals in the aliphatic region of the ^{1}H and ^{13}C spectra of acid **15** (Fig. 45S in Supplementary Material).

A single-crystal X-ray diffraction study of hybrid ligand **15** has been conducted in order to gain information on its solid-state structure. Crystals suitable for this study have been grown in DMSO by slow crystallization. The structure obtained for imidazole–acid **15** is shown in Fig. 5. This compound crystalizes in *Cc* space group of monoclinic system, and its molecular structure comprises neutral units of **15** and DMSO as solvate molecules in a 1:2 stoichiometric ratio. The analysis of the intermolecular hydrogen bonding has revealed the presence of a one-dimensional chain motif running along crystallographic axis *b*. A view of this 1D supramolecular aggregate is shown in Fig. 6. The 1D chain is further involved in intermolecular

hydrogen bonding interactions with co-crystallized DMSO molecules via formation of C-H···O contacts.

Conclusions

Our considered synthetic strategy efficiently led to the preparation of four hitherto unknown, structurally diverse, novel ligands with a pyrazole ring in the central unit to be subsequently used for the generation of coordination polymers. Unlike other synthetic strategies which rely heavily on palladium-based coupling chemistry for the preparation of carboxylate ligands, this approach is grounded on the facile Knorr pyrazole ring closure as the key step in the construction of the carboxylate-substituted central unit. For three of these target compounds, the investigated methodology could afford straightforward access to these ligands on multi-gram scale. NMR investigations showed that the enolic form is preferred for the two 4-aryl-2,4-oxobutanoates employed in these reactions, and demonstrated that hydroxypyrazoline is an intermediate in the formation of an N-1 unsubstituted pyrazole. For these N-1 unsubstituted pyrazoles, annular prototropic tautomerism could be evidenced in the case of an ester, but it was no longer noticeable in the case of the corresponding acid. Formation of 1,5-diarylpyrazoles as major regioisomers in the Knorr reaction of 4-aryl-2,4-oxobutanoates with phenylhydrazine was proved by NMR and also using single-crystal X-ray diffraction.

Experimental

Materials and instrumentation

All chemicals were purchased from commercial suppliers (Sigma–Aldrich, Steinheim, Germany; TCI Europe N.V., Zwijndrecht, Belgium; Merck KGaA, Darmstadt, Germany) and used without further purification. Melting points were taken on a Mel Temp II apparatus and are uncorrected. Elemental analysis was conducted in-house, on a PerkinElmer 2400 Series II CHNS/O system. Analytical TLC was run on Macherey–Nagel (Düren, Germany) aluminum-backed sheets that were precoated with silica gel 60 (0.20 mm thickness) containing fluorescence indicator UV_{254}, and the spots were visualized by UV illumination (254 nm). Column chromatography was performed on silica gel (230–400 mesh ASTM, 60 Å) (Merck, Darmstadt, Germany). A Bruker Vertex 70 spectrometer (Bruker Optik GmbH, Bremen, Germany) was used for the Fourier transform infrared (FTIR) spectra recording in the attenuated total reflection (ATR) configuration. All spectra were collected at a 2 cm^{-1} resolution, in the mid-IR range (4000–600 cm^{-1}). NMR spectra were recorded on two Bruker Avance NEO spectrometers (at 400 MHz, with a 5-mm probe for direct detection of H, C, F, Si, or at 600 MHz, with a 5-mm probe for inverse multinuclear detection). The exact signal assignments in both proton and carbon spectra were based mainly on proton–carbon correlation experiments, such as H,C-HSQC (heteronuclear single quantum coherence) and H,C-HMBC (heteronuclear multiple

bond correlation). The residual signals of the deuterated solvents were used as internal standard ($CDCl_3$: $\delta = 7.26$ ppm for ^1H and $\delta = 77.01$ ppm for ^{13}C; DMSO-d_6: $\delta = 2.51$ ppm for ^1H and $\delta = 39.47$ ppm for ^{13}C). The numbering of carbon atoms for each structure is shown in the corresponding spectra in Supplementary Material.

Synthesis

Claisen condensation of 4-acetylbenzonitrile (1) with diethyl oxalate

To a solution of sodium ethoxide, obtained by reacting sodium (1.38 g, 60 mmol) with abs. ethanol (60 mL), 4-acetylbenzonitrile (4.35 g, 30 mmol) and diethyl oxalate (8.76 g, 60 mmol) were sequentially added. The mixture was heated at reflux temperature for 2 h; then, it was cooled to room temperature and poured in a mixture of ice and water (700 g). The solid resulted after the mixture was brought to pH 2–3 by dropwise addition of 10% HCl was filtered, washed thoroughly with water, and air-dried. The crude compound was dissolved in chloroform (50 mL), and a small amount of insoluble material was filtered off. Removal of chloroform under reduced pressure and recrystallization of the resulting solid from 96% ethanol afforded diketoester **2** as tan crystals (5.51 g, 75%), mp 135–136 °C; ^1H NMR ($CDCl_3$, 400 MHz): δ 1.41 (3H, t, $J = 7.2$ Hz, CH_3), 4.41 (2H, q, $J = 7.2$ Hz, CH_2), 7.06 (1H, s, vinylic H), 7.80 (2H, d, $J = 8.0$ Hz, H-3), 8.07 (2H, d, $J = 8.0$ Hz, H-2), 14.95 (1H, br s, OH); ^{13}C NMR ($CDCl_3$, 100 MHz): δ 14.04 (CH_3), 62.89 (CH_2), 97.93 (vinylic CH), 116.72 (C-4), 117.74 (CN), 128.15 (CH-2), 132.62 (CH-3), 138.22 (C-1), 161.62 (COO), 172.19 (C-3′), 187.29 (C-1′); *Anal.* Calcd. for $C_{13}H_{11}NO_4$: C, 63.67; H, 4.52; N, 5.71. Found: C, 63.41; H, 4.41; N, 5.80.

One-pot synthesis of ethyl 3(5)-(4-cyanophenyl)-1H-pyrazole-5(3)-carboxylate (4)

To a suspension of diketoester **2** (735 mg, 3 mmol) in abs. ethanol (20 mL), hydrazine hydrate (150 mg, 3 mmol) was added, and the reaction mixture was stirred at room temperature for 48 h. Conc. H_2SO_4 (3–4 drops) was then added, and the mixture was heated at reflux temperature for 2 h. After a small amount of insoluble material had been filtered off, the solvent in the filtrate was removed under reduced pressure to give a solid material that was triturated with cold 2-propanol (5 mL). The solid was filtered, washed with water (2×10 mL), and air-dried to yield 470 mg (65%) of practically pure **4**. The material was recrystallized from 96% ethanol to afford the title compound as yellow crystals (360 mg, 50%), mp 214–215 °C; NMR data for the major tautomer: ^1H NMR (DMSO-d_6, 400 MHz): δ 1.34 (3H, t, $J = 7.2$ Hz, CH_3), 4.36 (2H, q, $J = 7.1$ Hz, CH_2), 7.51 (1H, d, $J = 1.5$ Hz, H-4), 7.88 (2H, d, $J = 8.3$ Hz, H-3′), 8.09 (2H, d, $J = 8.3$ Hz, H-2′), 14.31 (1H, s, NH); ^{13}C NMR (DMSO-d_6, 100 MHz): δ 14.12 (CH_3), 60.97 (CH_2), 106.75 (CH-4), 110.15 (C-4′), 118.85 (CN), 125.84 (CH-2′), 132.75 (CH-3′), 135.14 (C-5), 137.04 (C-1′), 149.57 (C-3), 158.80 (COO); NMR data for the minor tautomer: ^1H-NMR (DMSO-d_6, 400 MHz): δ 1.32 (3H, t, $J = 7.7$ Hz, CH_3), 4.31 (2H, q, $J = 7.2$ Hz, CH_2), 7.42 (1H, br s, H-4), 7.96 (2H, d, $J = 8.3$ Hz, H-3′), 8.04 (2H, d, $J = 8.3$ Hz, H-2′), 14.20 (1H, s, NH); ^{13}C-NMR (DMSO-d_6, 100 MHz): δ 14.20 (CH_3), 60.23 (CH_2),

106.60 (CH-4), 110.77 (C-4′), 118.57 (CN), 125.89 (CH-2′), 132.57 (C-1′), 133.06 (CH-3′), 141.74 (C-5), 144.36 (C-3), 161.74 (COO); *Anal.* Calcd. for $C_{13}H_{11}N_3O_2$: C, 64.72; H, 4.60; N, 17.42. Found: C, 64.47; H, 4.68; N, 17.22.

Preparation of 3(5)-(4-carboxyphenyl)-1H-pyrazole-5(3)-carboxylic acid (5)

Ethyl 3(5)-(4-cyanophenyl)-1*H*-pyrazole-5(3)-carboxylate (**4**) (241 mg, 1 mmol) was suspended in a solution of NaOH (120 mg, 3 mmol) in water (20 mL), and the mixture was heated at reflux temperature for 48 h. The slightly turbid liquid was filtered; then, the resulting solution was treated dropwise under efficient stirring with 5% acetic acid until pH is acidic. The fine precipitate was filtered, washed thoroughly with water, air-dried, and finally dried at 40–60 °C under medium vacuum overnight to afford the diacid **5** as colorless microcrystals (212 mg, 92%), mp > 300 °C; ^{1}H NMR (DMSO-d_6 + TFA, 400 MHz): δ 7.32 (1H, s, H-4), 7.96–8.01 (4H, m, H-2′ and H-3′), 10.7 (3H, br s, OH and NH overlaped with the TFA proton); ^{13}C NMR (DMSO-d_6 + TFA, 100 MHz): δ 106.29 (CH-4), 125.33 (CH-2′), 130.03 (CH-3′), 130.14 (C-4′), 135.67 (C-1′), 139.10 (C-5), 147.82 (C-3), 161.43 (pyrazole COO), 167.15 (phenyl COO); *Anal.* Calcd. for $C_{11}H_8N_2O_4$: C, 56.90; H, 3.47; N, 12.06. Found: C, 56.58; H, 3.61; N, 11.93.

Knorr synthesis of ethyl 5-(4-cyanophenyl)-1-phenyl-1H-pyrazole-3-carboxylate (6)

To a warm solution of diketoester **2** (4.9 g, 20 mmol) in glacial acetic acid (30 mL), phenylhydrazine (2.16 g, 20 mmol) was added dropwise under efficient stirring, and the mixture was heated at reflux temperature for 5 h. After it was allowed to reach room temperature, the mixture was added dropwise, under vigorous stirring, to a mixture of ice and water (400 g). The resulting solid was filtered and washed with plenty of water. When the material did not solidify when it was poured onto water, the semisolid was allowed to turn into a solid in the following one or 2 days, and then, it was filtered and washed with water. The solid material was recrystallized repeatedly (usually 2 or 3 times) from 96% ethanol until the presence of the minor regioisomer could no longer be detected by proton NMR. Yellowish crystals (3.93 g, 62%), mp 127–128 °C; ^{1}H NMR (DMSO-d_6, 400 MHz): δ 1.33 (3H, t, J = 7.1 Hz, CH_3), 4.35 (2H, q, J = 7.1 Hz, CH_2), 7.31 (1H, s, H-4), 7.35–7.36 (2H, m, H-2″), 7.46 (2H, d, J = 8.4 Hz, H-2′), 7.48–7.50 (3H, m, H-3″ and H-4″), 7.85 (2H, d, J = 8.4 Hz, H-3′); ^{13}C NMR (DMSO-d_6, 100 MHz): δ 14.18 (CH_3), 60.61 (CH_2), 110.60 (CH-4), 111.31 (C-4′), 118.29 (CN), 125.74 (CH-2″), 129.07 (CH-4″), 129.34, 129.43 (CH-3″ and CH-2′), 132.49 (CH-3′), 133.29 (C-1′), 138.82 (C-1″), 142.61 (C-5), 143.67 (C-3), 161.34 (COO); *Anal.* Calcd. for $C_{19}H_{15}N_3O_2$: C, 71.91; H, 4.76; N, 13.24. Found: C, 71.68; H, 4.93; N, 13.47.

Preparation of 5-(4-carboxyphenyl)-1-phenyl-1H-pyrazole-3-carboxylic acid (7)

Ethyl 5-(4-cyanophenyl)-1-phenyl-1*H*-pyrazole-3-carboxylate (**6**) (475 mg, 1.5 mmol) was suspended in a solution of NaOH (180 mg, 4.5 mmol) in water (20 mL), and the mixture was heated at reflux temperature for 48 h. The cold reaction mixture was filtered to remove a small amount of solid, and then, the resulting

solution was brought to pH 5–6 by dropwise addition of 5% acetic acid under efficient stirring. The fine precipitate was filtered, washed with plenty of water, air-dried, and finally dried at 40–60 °C under medium vacuum overnight to afford compound **7** as colorless microcrystals (385 mg, 83%), mp 248–249 °C (dec.); ^{1}H NMR (DMSO-d_6, 400 MHz): δ 7.19 (1H, s, H-4), 7.33-7.36 (2H, m, H-2″), 7.38 (2H, d, J = 8.3 Hz, H-2′), 7.45-7.49 (3H, m, H-3″ and H-4″), 7.90 (2H, d, J = 8.3 Hz, H-3′), 13.33 (2H, br s, OH); ^{13}C NMR (DMSO-d_6, 100 MHz): δ 110.29 (CH-4), 125.61 (CH-2″), 128.75 (CH-2′), 129.33 (CH-3″ and CH-4″), 129.46 (CH-3′), 130.71 (C-4′), 133.13 (C-1′), 139.08 (C-1″), 143.21 (C-5), 144.54 (C-3), 162.89 (pyrazole COO), 166.71 (phenyl COO); *Anal.* Calcd. for $C_{17}H_{12}N_2O_4$: C, 66.23; H, 3.92; N, 9.09. Found: C, 66.01; H, 4.08; N, 8.95.

Mild hydrolysis of ester 6 to 5-(4-cyanophenyl)-1-phenyl-1H-pyrazole-3-carboxylic acid (8)

Ethyl 5-(4-cyanophenyl)-1-phenyl-1*H*-pyrazole-3-carboxylate (**6**) (317 mg, 1 mmol) and LiOH (48 mg, 2 mmol) in a mixture of THF–methanol–water (5 mL, 3:1:1, *v*/*v*/*v*) were stirred at room temperature overnight. A small amount of insoluble material was removed by filtration; then, the solution was diluted with water (45 mL) and treated dropwise with 10% HCl until pH reached 2–3. The fine precipitate was filtered, washed thoroughly with water, air-dried, and finally dried at 40–60 °C under medium vacuum overnight to afford compound **8** as colorless microcrystals (270 mg, 93%), mp 215–216 °C (dec.); ^{1}H NMR (DMSO-d_6, 400 MHz): δ 7.26 (1H, s, H-4), 7.34–7.37 (2H, m, H-2″), 7.45 (2H, d, J = 8.4 Hz, H-2′), 7.48–7.50 (3H, m, H-3″ and H-4″), 7.85 (2H, d, J = 8.3 Hz, H-3′), 13.10 (1H, br s, OH); ^{13}C NMR (DMSO-d_6, 100 MHz): δ 110.71 (CH-4), 111.23 (C-4′), 118.35 (CN), 125.71 (CH-2″), 128.95 (CH-4″), 129.35, 129.42 (CH-3″ and CH-2′), 132.51 (CH-3′), 133.52 (C-1′), 138.93 (C-1″), 142.47 (C-5), 144.67 (C-3), 162.84 (COO); *Anal.* Calcd. for $C_{17}H_{11}N_3O_2$: C, 70.58; H, 3.83; N, 14.53. Found: C, 70.39; H, 3.98; N, 14.34.

Tetrazole ring closure—isolation of ethyl 5-[4-(1H-tetrazol-5-yl) phenyl]-1-phenyl-1H-pyrazole-3-carboxylate (9)

A mixture of ethyl 5-(4-cyanophenyl)-1-phenyl-1*H*-pyrazole-3-carboxylate (**6**) (951 mg, 3 mmol), NaN_3 (683 mg, 10.5 mmol), and NH_4Cl (402 mg, 7.5 mmol) in DMF (10 mL) was heated at 120 °C (oil bath temperature) for 48 h. The cold reaction mixture was poured slowly, under efficient stirring and in a thin stream in ice–water (150 g). The precipitate was filtered, washed with water (3 × 30 mL), and air-dried to give a colorless solid (575 mg), which was recrystallized from 96% ethanol to afford ester **9** as off-white crystals (410 mg), mp 224–225 °C (dec.); ^{1}H NMR (DMSO-d_6, 400 MHz): δ 1.33 (3H, t, J = 7.1 Hz, CH_3), 4.36 (2H, q, J = 7.1 Hz, CH_2), 7.27 (1H, s, H-4), 7.38-7.40 (2H, m, H-2″), 7.48-7.51 (5H, m, H-2′, H-3″ and H-4″), 8.00 (2H, d, J = 8.4 Hz, H-3′), 16.96 (1H, br s, NH); ^{13}C NMR (DMSO-d_6, 100 MHz): δ 14.18 (CH_3), 60.55 (CH_2), 110.09 (CH-4), 124.35 (C-4′), 125.70 (CH-2″), 127.09 (CH-3′), 128.90 (CH-4″), 129.36, and 129.49 (CH-3″ and CH-2′), 131.33 (C-1′), 138.99 (C-1″), 143.28 (C-5), 143.60 (C-3), 155.05 (C-5‴), 161.42

(COO); *Anal.* Calcd. for $C_{19}H_{16}N_6O_2$: C, 63.32; H, 4.48; N, 23.32. Found: C, 63.09; H, 4.55; N, 23.51.

When the filtrate from the isolation of the aforementioned colorless solid was treated with excess 10% acetic acid, a colorless fine solid separated out. The material was filtered, washed with water (3 × 30 mL), and air-dried to give a solid (385 mg), which was recrystallized from 96% ethanol to afford a second crop of ester **9** (227 mg), having the same melting point as the first crop, the same mixed melting point, and the same NMR spectra as the first crop. The total yield of pure compound **9** isolated from this experiment was 59%.

Tetrazole ring closure—isolation of a mixture of ester 9 and corresponding acid 10

A mixture of ethyl 5-(4-cyanophenyl)-1-phenyl-1*H*-pyrazole-3-carboxylate (**6**) (951 mg, 3 mmol), NaN_3 (683 mg, 10.5 mmol), and NH_4Cl (402 mg, 7.5 mmol) in *N*,*N*-dimethylformamide (10 mL) was heated at 120 °C (oil bath temperature) for 48 h. The cold reaction mixture was poured in ice–water (150 g), and then, the pH of the mixture was brought to 2–3 by addition of 36% HCl. The precipitate was washed with water (3 × 30 mL) and air-dried to give a mixture of ester **9** and acid **10** (1025 mg). NMR analysis showed that the ratio between ester **9** and acid **10** is approximately 12 to 1.

Synthesis of 5-[4-(1H-tetrazol-5-yl)phenyl]-1-phenyl-1H-pyrazole-3-carboxylic acid (10) by hydrolysis of pure ester 9

Ethyl 5-[4-(1*H*-tetrazol-5-yl)phenyl]-1-phenyl-1*H*-pyrazole-3-carboxylate (**9**) (540 mg, 1.5 mmol) and LiOH (108 mg, 4.5 mmol) were stirred in a mixture of THF–methanol–water (10 mL, 3:1:1, *v*/*v*/*v*) at room temperature overnight. The mixture was then diluted with water (40 mL) and treated dropwise with 10% HCl until pH reached 2–3. The precipitate was filtered, washed with water (3 × 30 mL), air-dried, and finally dried at 40–60 °C under medium vacuum overnight to give colorless microcrystals (490 mg, 98%), mp 269–270 °C (dec.); ^{1}H NMR (DMSO-d_6, 400 MHz): δ 7.22 (1H, s, H-4), 7.37–7.39 (2H, m, H-2″), 7.48–7.50 (5H, m, H-2′, H-3″ and H-4″), 8.00 (2H, d, J = 8.2 Hz, H-3′), 13.09 (1H, br s, OH), 16.95 (1H, br s, NH); ^{13}C NMR (DMSO-d_6, 100 MHz): δ 110.22 (CH-4), 124.28 (C-4′), 125.67 (CH-2″), 127.12 (CH-3′), 128.79 (CH-4″), 129.35 (CH-2′), 129.52 (CH-3″), 131.58 (C-1′), 139.10 (C-1″), 143.15 (C-5), 144.53 (C-3), 154.96 (C-5‴), 162.90 (COO); *Anal.* Calcd. for $C_{17}H_{12}N_6O_2$: C, 61.44; H, 3.64; N, 25.29. Found: C, 61.22; H, 3.73; N, 25.11.

Preparation of 5-[4-(2H-tetrazol-5-yl)phenyl]-1-phenyl-1H-pyrazole-3-carboxylic acid (10) by hydrolysis of a mixture of ester 9 and acid 10

The previously isolated mixture of ester **9** and acid **10** (1025 mg) was suspended in a solution of NaOH (360 mg) in water (25 mL) and heated at reflux temperature for 10 h. The cold reaction mixture was filtered, diluted with water (25 mL), and acidified with 10% HCl. The precipitate was filtered, washed with water (3 × 30 mL), air-dried, and finally dried at 40–60 °C under medium vacuum overnight to give

colorless microcrystals (840 mg, 89%), which had the same melting point as acid **10** obtained through the hydrolysis of pure ester **9**, the same mixed melting point, and the same NMR spectra as the sample obtained from the hydrolysis of pure ester **9**.

Claisen condensation of 4-(1H-imidazol-1-yl)acetophenone (11) with diethyl oxalate

4-(1*H*-Imidazol-1-yl)acetophenone (**11**) (1488 mg, 8 mmol) and diethyl oxalate (2336 mg, 16 mmol) were added to a solution of sodium ethoxide, previously obtained by reacting sodium (368 mg, 16 mmol) with abs. ethanol (60 mL). The reaction mixture was heated at reflux temperature for 2 h, and then, it was poured onto a mixture of ice and water (500 g) and brought to acidic pH by addition of 10% acetic acid. The solid was filtered, washed thoroughly with water, and air-dried to give diketoester **12** as a yellow solid (1945 mg, 85%) which was deemed pure enough for the next step by NMR analysis. The analytical sample was recrystallized from ethanol to give yellow crystals, mp 123–124 °C (darkening, dec.); ^{1}H NMR ($CDCl_3$, 400 MHz): δ 1.42 (3H, t, J = 7.2 Hz, CH_3), 4.41 (2H, q, J = 7.1 Hz, CH_2), 7.08 (1H, s, H-2′), 7.25 (1H, br s, imidazole H-4), 7.37 (1H, br s, imidazole H-5), 7.54 (2H, d, J = 8.7 Hz, H-3), 7.97 (1H, br s, imidazole H-2), 8.13 (2H, d, J = 8.7 Hz, H-2), 14.87 (1H, br s, OH); ^{13}C NMR ($CDCl_3$, 100 MHz): δ 14.07 (CH_3), 62.75 (CH_2), 97.77 (vinylic CH), 117.60 (imidazole CH-5), 120.88 (CH-3), 129.89 (CH-2), 131.27 (imidazole CH-4), 133.56 (C-1), 135.32 (imidazole CH-2), 141.18 (C-4), 162.01 (COO), 170.14 (C-3′), 188.88 (C-1′); *Anal.* Calcd. for $C_{15}H_{14}N_2O_4$: C, 62.93; H, 4.93; N, 9.79. Found: C, 63.11; H, 4.81; N, 9.91.

Ethyl 5-[4-(1H-imidazol-1-yl)phenyl]-1-phenyl-1H-pyrazole-3-carboxylate (13) and ethyl 3-[4-(1H-imidazol-1-yl)phenyl]-1-phenyl-1H-pyrazole-5-carboxylate (14) through pyrazole ring formation

A mixture consisting of diketoester **12** (858 mg, 3 mmol) and phenylhydrazine (328 mg, 3 mmol) in glacial acetic acid (10 mL) was heated at reflux temperature for 5 h. The cold mixture was added dropwise to ice–water (150 g), and then, the resulting solution was brought to pH 8 by addition of 10% NaOH. The brownish semisolid is allowed to become solid over the weekend; then, the material is filtered, washed with water (3×30 mL), and air-dried. Column chromatography (ethyl acetate–*n*-hexane, 1:1 *v*/*v*) allowed the separation of the minor component **14** (45 mg, 4%) as an off-white solid, mp 140–141 °C, R_f 0.11 (ethyl acetate–*n*-hexane, 1:1 *v*/*v*); ^{1}H NMR ($CDCl_3$, 600 MHz): δ 1.27 (3H, t, J = 7.1 Hz, CH_3), 4.27 (2H, q, J = 7.1 Hz, CH_2), 7.22 (1H, t, J = 0.9 Hz, imidazole H-4), 7.32 (1H, t, J = 1.3 Hz, imidazole H-5), 7.35 (1H, s, H-4), 7.45 (2H, d, J = 8.7 Hz, H-3′), 7.47–7.50 (5H, m, H-2″, H-3″ and H-4″), 7.91 (1H, t, J = 0.9 Hz, imidazole H-2), 7.99 (2H, d, J = 8.8 Hz, H-2′); ^{13}C NMR ($CDCl_3$, 151 MHz): δ 14.02 (CH_3), 61.35 (CH_2), 109.38 (CH-4), 118.09 (imidazole CH-5), 121.59 (CH-3′), 126.08 (CH-2″), 127.22 (CH-2′), 128.66 (CH-3″), 128.87 (CH-4″), 130.53 (imidazole CH-4), 131.55 (C-1′), 135.01 (C-5), 135.49 (imidazole CH-2), 137.15 (C-4′), 140.24 (C-1″), 150.13 (C-3), 158.95 (COO); *Anal.* Calcd. for $C_{21}H_{18}N_4O_2$: C, 70.38; H, 5.06; N, 15.63. Found: C, 70.62; H, 4.97; N, 15.52.

Further elution with ethyl acetate–*n*-hexane (1:1 *v*/*v*) yielded fractions containing the major component **13** (685 mg, 64%) as a tan solid, mp 147–148 °C, R_f 0.06 (ethyl

acetate–*n*-hexane, 1:1 *v*/*v*); ^{1}H NMR ($CDCl_3$, 600 MHz): δ 1.42 (3H, t, J=7.1 Hz, CH_3), 4.46 (2H, q, J=7.1 Hz, CH_2), 7.09 (1H, s, H-4), 7.20 (1H, t, J=1.0 Hz, imidazole H-4), 7.27 (1H, t, J=1.3 Hz, imidazole H-5), 7.31–7.36 (6H, m, H-2′, H-3′ and H-2″), 7.37–7.40 (3H, m, H-3″ and H-4″), 7.86 (1H, t, J=1.0 Hz, imidazole H-2); ^{13}C NMR ($CDCl_3$, 151 MHz): δ 14.38 (CH_3), 61.24 (CH_2), 110.10 (CH-4), 117.80 (imidazole CH-5), 121.22 (CH-3′), 125.78 (CH-2″), 128.61 (C-1′), 128.69 (CH-4″), 129.19 (CH-3″), 130.20 (CH-2′), 130.81 (imidazole CH-4), 135.33 (imidazole CH-2), 137.33 (C-4′), 139.27 (C-1″), 143.20 (C-5), 144.51 (C-3), 162.23 (COO); *Anal.* Calcd. for $C_{21}H_{18}N_4O_2$: C, 70.38; H, 5.06; N, 15.63. Found: C, 70.57; H, 5.14; N, 15.75.

The corresponding hydrochloride **13**·HCl was obtained as colorless microcrystals, mp 230–231 °C (dec.); ^{1}H NMR (DMSO-d_6, 400 MHz): δ 1.34 (3H, t, J=7.1 Hz, CH_3), 4.36 (2H, q, J=7.1 Hz, CH_2), 7.30 (1H, s, H-4), 7.40–7.42 (2H, m, H-2″), 7.49–7.54 (5H, m, H-2′, H-3″ and H-4″), 7.86 (2H, d, J=8.7 Hz, H-3′), 7.90 (1H, t, J=1.5 Hz, imidazole H-4), 8.32 (1H, t, J=1.6 Hz, imidazole H-5), 9.76 (1H, t, J=1.2 Hz, imidazole H-2), 15.36 (1H, br s, NH^+); ^{13}C NMR (DMSO-d_6, 100 MHz): δ 14.20 (CH_3), 60.58 (CH_2), 110.15 (CH-4), 120.38 (imidazole CH-5), 121.25 (imidazole CH-4), 121.82 (CH-3′), 125.92 (CH-2″), 129.05 (CH-4″), 129.43 (CH-3″), 129.69 (C-1′), 130.09 (CH-2′), 134.58 (imidazole CH-2), 134.95 (C-4′), 139.01 (C-1″), 142.91 (C-5), 143.55 (C-3), 161.45 (COO); *Anal.* Calcd. for $C_{21}H_{19}ClN_4O_2$: C, 63.88; H, 4.85; N, 14.19. Found: C, 64.16; H, 4.95; N, 14.43.

Hydrolysis of ester 13 to 5-[4-(1H-imidazol-1-yl) phenyl]-1-phenyl-1H-pyrazole-3-carboxylic acid (15)

Ester **13** (358 mg, 1 mmol) and LiOH (72 mg, 3 mmol) were stirred in a mixture of THF–methanol–water (10 mL, 3:1:1, *v*/*v*/*v*) at room temperature overnight. After dilution with water (40 mL), the solution was treated dropwise with 10% acetic acid until pH 5–6. The fine precipitate was filtered, washed with water (3×30 mL), air-dried, and finally dried at 40–60 °C under medium vacuum overnight to give colorless microcrystals (300 mg, 91%), mp 278–279 °C (dec.); ^{1}H NMR (DMSO-d_6, 400 MHz): δ 7.12 (1H, br s, imidazole H-4), 7.17 (1H, s, H-4), 7.38–7.41 (4H, m, H-2′ and H-2″), 7.48-7.50 (3H, m, H-3″ and H-4″), 7.69 (2H, d, J=8.6 Hz, H-3′), 7.81 (1H, br s, imidazole H-5), 8.33 (1H, br s, imidazole H-2), 13.05 (1H, br s, OH); ^{13}C NMR (DMSO-d_6, 100 MHz): δ 109.80 (CH-4), 117.68 (imidazole CH-5), 119.94 (CH-3′), 125.75 (CH-2″), 127.28 (C-1′), 128.75 (CH-4″), 129.32 (CH-3″), 130.00 (CH-2′), 130.06 (imidazole CH-4), 135.45 (imidazole CH-2), 136.81 (C-4′), 139.23 (C-1″), 143.20 (C-5), 144.41 (C-3), 162.97 (COO); *Anal.* Calcd. for $C_{19}H_{14}N_4O_2$: C, 69.08; H, 4.27; N, 16.96. Found: C, 68.89; H, 4.41; N, 16.78. The same compound could be obtained in 87% yield by a similar procedure that used **13**·HCl as substrate and 4 equivalents of LiOH.

X-ray crystallography

X-ray diffraction measurements were carried out with an Oxford Diffraction XCALIBUR E CCD diffractometer equipped with graphite-monochromated MoKα radiation. Single crystals were positioned at 40 mm from the detector, and 369, 215, and 736

frames were measured each for 80, 125, and 5 s over 1° scan width for **6**, **10,** and **15**, respectively. The unit cell determination and data integration were carried out using the CrysAlis package of Oxford Diffraction [46]. The structures were solved by direct methods using Olex2 [47] and refined by full-matrix least squares on F^2 with SHELXL-97 [48] using an anisotropic model for non-hydrogen atoms. All H-atoms were placed in calculated positions (d_{CH} = 0.93 Å) and refined as riding with $U_{iso}(H) = 1.2U_{iso}(C)$. The positional parameters of disordered DMSO molecules in **15** were refined using available tools (PART, DFIX, and SADI) of SHELXL97. The molecular plots were obtained using the Olex2 program. The crystallographic data and refinement details are presented in Table 1, while bond lengths and angles are summarized in Table S1 (Supplementary Material). CCDC-1942897 (**6**), CCDC-1942898 (**10**), and CCDC-1942903 (**15**) contain the supplementary crystallographic data for this contribution. These data can be obtained free of charge via www.ccdc.cam.ac.uk/conts/retrieving.html (or from

Table 1 Crystal data and details of data collection for **6**, **10,** and **15**

Compound	**6**	**10**	**15**
Empirical formula	$C_{19}H_{15}N_3O_2$	$C_{17}H_{12}N_6O_2$	$C_{23}H_{26}N_4O_4S_2$
Fw	317.34	332.33	486.60
Space group	*P*-1	$P2_12_12_1$	*Cc*
a (Å)	8.5642(6)	5.9614(7)	10.3034(3)
b (Å)	9.3634(6)	8.8381(10)	14.6606(3)
c (Å)	11.3812(7)	28.489(4)	16.2154(4)
α (°)	77.961(6)	90	90
β (°)	69.328(6)	90	96.814(3)
γ (°)	83.693(6)	90	90
V (Å^3)	834.47(10)	1501.0(3)	2432.09(12)
Z	2	4	4
λ (Å)	0.71073	0.71073	0.71073
ρ_{calcd} (g cm^{-3})	1.263	1.471	1.329
Crystal size (mm)	0.35 × 0.3 × 0.25	0.40 × 0.10 × 0.05	0.35 × 0.25 × 0.15
T (K)	200	180	180
μ (mm^{-1})	0.084	0.103	0.255
2Θ range	3.89 to 50.05	5.424 to 50.05	4.856 to 49.426
Reflections collected	5369	5102	14,519
Independent reflections	2934 [R_{int} = 0.0217]	2646 [R_{int} = 0.0501]	4148 [R_{int} = 0.0371]
Data/restraints/parameters	2934/0/218	2646/0/227	4148/63/318
R_1^a	0.0453	0.0600	0.0783
wR_2^b	0.1006	0.0827	0.2257
GOF[c]	1.048	1.003	1.028
Largest diff. peak/hole/e Å^{-3}	0.14/−0.23	0.22/−0.23	1.01/−0.68
Flack parameter	–	–	0.01(5)

[a] $R_1 = \Sigma||F_o| - |F_c||/\Sigma|F_o|$

[b] $wR_2 = \{\Sigma[w(F_o^2 - F_c^2)^2]/\Sigma[w(F_o^2)^2]\}^{1/2}$

[c] $GOF = \{\Sigma[w(F_o^2 - F_c^2)^2]/(n-p)\}^{1/2}$, where *n* is the number of reflections and *p* is the total number of parameters refined

the Cambridge Crystallographic Data Centre, 12 Union Road, Cambridge CB2 1EZ, UK; fax: (+44) 1223-336-033; or deposit@ccdc.ca.ac.uk).

Acknowledgements The financial support of European Social Fund for Regional Development, Competitiveness Operational Programme Axis 1—Project "Novel Porous Coordination Polymers with Organic Ligands of Variable Length for Gas Storage," POCPOLIG (ID P_37_707, Contract 67/08.09.2016, cod MySMIS: 104810) is gratefully acknowledged.

References

1. Y. Lin, C. Kong, Q. Zhang, L. Chen, Adv. Energy Mater. **7**, 1601296 (2017)
2. H. Li, K. Wang, Y. Sun, C.T. Lollar, J. Li, H.-C. Zhou, Mater. Today **21**, 108 (2018)
3. X. Yang, Q. Xu, Cryst. Growth Des. **17**, 1450 (2017)
4. L. Zhu, X.-Q. Liu, H.-L. Jiang, L.-B. Sun, Chem. Rev. **117**, 8129 (2017)
5. C. Janiak, J.K. Vieth, New J. Chem. **34**, 2366 (2010)
6. Z.-Q. Shi, Z.-J. Guo, H.-G. Zheng, Chem. Commun. **51**, 8300 (2015)
7. H. Erer, O.Z. Yeşilel, M. Arici, S. Keskin, O. Büyükgüngör, J. Solid State Chem. **210**, 261 (2014)
8. H.-H. Li, Z. Niu, L. Chen, H.-B. Jiang, Y.-P. Wang, P. Cheng, CrystEngComm **17**, 5101 (2015)
9. R. Sen, D. Mal, P. Brandão, G. Rogez, Z. Lin, CrystEngComm **15**, 2113 (2013)
10. S. Demir, H.M. Çepni, N. Bilgin, M. Hołyńska, F. Yilmaz, Polyhedron **115**, 236 (2016)
11. I. Voda, G. Makhloufi, V. Druta, V. Lozan, S. Shova, P. Bourosh, V. Kravtsov, C. Janiak, Inorg. Chim. Acta **482**, 526 (2018)
12. Y. Zhang, X. Luo, Z. Yang, G. Li, CrystEngComm **14**, 7382 (2012)
13. Z.-G. Gu, Y.-T. Liu, X.-J. Hong, Q.-G. Zhan, Z.-P. Zheng, S.-R. Zheng, W.-S. Li, S.-J. Hu, Y.-P. Cai, Cryst. Growth Des. **12**, 2178 (2012)
14. L. Bahrin, I. Rosca, L. Clima, S. Shova, D. Bejan, A. Nicolescu, N. Marangoci, M. Sardaru, V. Lozan, A. Rotaru, Inorg. Chem. Commun. **92**, 60 (2018)
15. D. Bejan, L.G. Bahrin, S. Shova, M. Sardaru, L. Clima, A. Nicolescu, N. Marangoci, V. Lozan, C. Janiak, Inorg. Chim. Acta **482**, 275 (2018)
16. I.-A. Dascalu, S. Shova, D.G. Dumitrescu, G. Roman, B.-I. Bratanovici, R. Ardeleanu, V. Lozan, Polyhedron **170**, 463 (2019)
17. L.G. Bahrin, D. Bejan, S. Shova, M. Gdaniec, M. Fronc, V. Lozan, C. Janiak, Polyhedron **173**, 114128 (2019)
18. Y.L. Janin, Mini Rev. Org. Chem. **7**, 314 (2010)
19. A.G. Waterson, J.P. Kennedy, J.D. Patrone, N.F. Pelz, M.D. Feldkamp, A.O. Frank, B. Vangamudi, E.M. Souza-Fagundes, O.W. Rossanese, W.J. Chazin, S.W. Fesik, ACS Med. Chem. Lett. **6**, 140 (2015)
20. H.R. Hoveyda, M.-O. Roy, S. Blanc, S. Noël, J.M. Salvino, M.A. Ator, G. Fraser, Bioorg. Med. Chem. Lett. **21**, 1991 (2011)
21. K. Tsuji, K. Nakamura, N. Konishi, T. Tojo, T. Ochi, H. Senoh, M. Matsuo, Chem. Pharm. Bull. **45**, 987 (1997)
22. T. Rogez-Florent, S. Meignan, C. Foulon, P. Six, A. Gros, C. Bal-Mahieu, C.T. Supuran, A. Scozzafava, R. Frédérick, B. Masereel, P. Depreux, A. Lansiaux, J.-F. Goossens, S. Gluszok, L. Goossens, Bioorg. Med. Chem. **21**, 1451 (2013)
23. J.N. Spencer, E.S. Holmboe, M.R. Kirshenbaudm, D.W. Firth, P.B. Pinto, Can. J. Chem. **60**, 1178 (1982)
24. V.R. Darugar, M. Vakili, A.R. Nekoei, S.F. Tayyari, R. Afzali, J. Mol. Struct. **1150**, 427 (2017)
25. S.P. Singh, D. Kumar, H. Batra, R. Naithani, I. Rozas, J. Elguero, Can. J. Chem. **78**, 1109 (2000). **(References cited therein)**
26. T. Norris, R. Colon-Cruz, D.H.B. Ripin, Org. Biomol. Chem. **3**, 1844 (2003)
27. A.V. Zerov, T.S. Krupenya, A.A. Petrov, S.I. Yakimovich, Russ. J. Org. Chem. **52**, 312 (2016)
28. R.M. Claramunt, C. Lopez, M.D. Santa Maria, D. Sanz, J. Elguero, Prog. Nucl. Magn. Reson. Spectrosc. **49**, 169 (2006)

29. D. Sanz, R.M. Claramunt, I. Alkorta, J. Elguero, W.R. Thiel, T. Ruffer, New J. Chem. **32**, 2225 (2008)
30. E.D. Doidge, J.W. Roebuck, M.R. Healy, P.A. Tasker, Coord. Chem. Rev. **288**, 98 (2015)
31. J. Klingele, S. Dechert, F. Meyer, Coord. Chem. Rev. **253**, 2698 (2009)
32. C. Pettinari, A. Tăbăcaru, S. Galli, Coord. Chem. Rev. **307**, 1 (2016)
33. W.V. Murray, M.P. Wachter, J. Heterocycl. Chem. **26**, 1389 (1989)
34. M.A. Tabrizi, P.G. Baraldi, E. Ruggiero, G. Saponaro, S. Baraldi, R. Romagnoli, A. Martinelli, T. Tuccinardi, Eur. J. Med. Chem. **97**, 289 (2015)
35. M. Alvarado, J. Decara, M.J. Luque, L. Hernandez-Folgado, M. Gómez-Cañas, M. Gómez-Ruiz, J. Fernández-Ruiz, J. Elguero, N. Jagerovic, A. Serrano, P. Goya, F. Rodríguez de Fonseca, Bioorg. Med. Chem. **21**, 1708 (2013)
36. I. Alkorta, M. Alvarado, J. Elguero, S. García-Granda, P. Goya, L. Torre-Fernández, L. Menéndez-Taboada, J. Mol. Struct. **920**, 82 (2009)
37. A.P. Kozikowski, S. Tapadar, D.N. Luchini, K.H. Kim, D.D. Billadeau, J. Med. Chem. **51**, 4370 (2008)
38. K. Liu, Y. Peng, F. Yang, D. Ma, G. Li, Z. Shi, S. Feng, CrystEngComm **16**, 4382 (2014)
39. S.-J. Bao, R. Krishna, Y.-B. He, J.-S. Qin, Z.-M. Su, S.-L. Li, W. Xie, D.-Y. Du, W.-W. He, S.-R. Zhang, Y.-Q. Lan, J. Mater. Chem. A **3**, 7361 (2015)
40. Y.-P. Xu, Y.-H. Chen, Z.-J. Chen, J. Qin, S.-S. Qian, H.-L. Zhu, Eur. J. Inorg. Chem. **2015**, 2076 (2015)
41. Y.-H. Mu, Z.-W. Ge, C.-P. Li, Inorg. Chem. Commun. **48**, 94 (2014)
42. C. Heering, I. Boldog, V. Vasylyeva, J. Sanchiz, C. Janiak, CrystEngComm **15**, 9757 (2013)
43. Y. Zhou, R. Ni, G. Yang, Synth. Commun. **40**, 2624 (2010)
44. V.I. Minkin, A.D. Garnovskii, J. Elguero, A.R. Katritzky, O.V. Denisko, Adv. Heterocycl. Chem. **76**, 157 (2000)
45. R. Ardeleanu, A. Dascălu, S. Shova, A. Nicolescu, I. Roşca, B.-I. Bratanovici, V. Lozan, G. Roman, J. Mol. Struct. **1173**, 63 (2018)
46. CrysAlisRED, Oxford Diffraction Ltd., Version 1.171.34.76 (2003)
47. O.V. Dolomanov, L.J. Bourhis, R.J. Gildea, J.A.K. Howard, H. Puschmann, J. Appl. Cryst. **42**, 339 (2009)
48. G.M. Sheldrick, Acta Crystallogr. C **71**, 3 (2015)